On the Reaction of FNO_2 with CH_3, *tert*-Butyl, and $C_{13}H_{21}$

H. T. Thümmel and C. W. Bauschlicher, Jr.*

NASA Ames Research Center, Moffett Field, California, 94035

Received: October 17, 1996⊗

Theoretical studies are reported for the reaction of FNO_2 with the radicals CH_3, *tert*-butyl, and $C_{13}H_{21}$, which are templates for the radical site of a hydrogenated diamond (111) surface. All structures are fully optimized using density functional theory based on the B3LYP functional. Calibration calculations are performed for $CH_3 + FNO_2$ using the coupled cluster approach, the internally contracted multireference configuration interaction method, and second-order perturbation theory based upon the complete-active-space SCF reference wave function. These calibration calculations support the B3LYP approach for the calculation of bond energies but show that the B3LYP barrier is too low. Combining the calibration calculations with the larger clusters yields our best estimate of a barrier of about 10 kcal/mol for the reaction of FNO_2 with a radical site on hydrogenated diamond (111).

1. Introduction

Data storage requirements continue to expand at an amazing rate, which has led people to consider many nonstandard techniques.[1] The highest data densities can be achieved by using atoms to store data. Positioning Xe atoms on a Ni surface is an example of such an idea,[2] but it is clearly impractical as the basis of a real data storage device. More recently a scanning tunneling microscope (STM) has been used to flip silicon dimers on a Si (100) surface;[3] the ultrahigh vacuum and low temperatures required to maintain the data and the long time to read and write the data currently make this, like the rare gas atoms on a metal surface, impractical as the basis of a data storage device.

The low-temperature requirement to maintain the data integrity can be removed by using strong covalent bonds to store the data. This has led us to propose[4] using H and F on a diamond (111) surface to store data. Both the C−H and C−F bonds are sufficiently strong that once formed, they should remain for long periods of time. An atomic force microscope (AFM) should be suitable for reading such data. Starting with a hydrogen passivated surface, the data could be written by replacing selected hydrogen atoms with fluorine atoms; unfortunately it is not obvious how to accomplish this substitution.

Recently Avouris and co-workers[5] have been investigating a similar surface data storage idea, except they have proposed Si instead of C. They have shown that by applying an electric field to an STM tip they can remove individual H atoms from a hydrogen passivated Si surface. If F atoms could be bonded to the Si surface at the site of each removed H atom, a stable surface encoded with the desired data would be formed. It is expected that the same technique could be used to remove H atoms from the diamond (111) surface. Therefore we have investigated methods for adding F atoms to the radical site on a diamond surface as a possible method of writing data on a diamond (111) surface.

We should note that there is also interest in forming a F-coated diamond surface as this is predicted to be a surface with very low friction. Yates and co-workers[6] have reported a method for adding F to a diamond (100) surface. Unfortunately this method does not simply add F to a diamond surface but rather adds C_nF_m, which upon heating forms a F-coated surface. It is possible that this approach could roughen the surface. Ideally one would like to selectively replace the H atoms on a hydrogenated diamond surface with F atoms, so that one could produce a F/diamond (111) surface with the same roughness as the original surface. Thus, in addition to data storage concerns, there is a potential tribology interest in selectively replacing the H atoms with F atoms on a diamond surface.

To selectively add fluorine to the surface, we need to avoid the formation of destructive radicals. For example, one could produce F atoms by decomposition of F_2, and some of the F radical would react with the surface radical sites, but others would abstract a hydrogen from the surface to form new surface radicals, which is clearly unacceptable for the data storage application. At high F concentrations, etching of the surface could result, which is undesirable. Thus it seems that a better starting point is a reasonably stable molecule, XF, that will react with a surface radical to produce a surface F, but one where the X radical produced after the F deposition will not abstract an H atom to produce an unwanted surface radical. Ideally the X should be sufficiently bulky that X does not bond to the surface or that at least the X−surface bond is extremely weak. Other desirable features are that there is a known synthesis for XF and that XF is a gas at reasonable temperatures, so that the F atoms can be added by exposing the surface to XF after, or while, the STM is being used to remove H atoms.

We investigated many XF compounds for these desired characteristics. When experimental bond energies were not available, *ab initio* calculations were performed. On the basis of an extensive search, FNO_2 and FNO appeared to be the best candidates for F deposition, and in this manuscript we report on calculations designed to test FNO_2 for this purpose. We should note that NO_2 is known to bond to a diamond surface, and if sufficient energy is added, for example by atomic bombardment, it will react with the surface and etch it.[7] Therefore, we envision the FNO_2 being used for low surface radical concentrations, where the NO_2 radical will be carried off before finding a radical site. However, it is possible that the NO_2 could be removed in the same way as the H atoms, so that unwanted NO_2 reactions could be corrected in a second writing phase. Anyone interested in the survey studies should contact one of the authors (H.T.T.) at thuemmel@pegasus.arc.nasa.gov.

⊗ Abstract published in *Advance ACS Abstracts,* January 15, 1997.

S1089-5639(96)03201-X

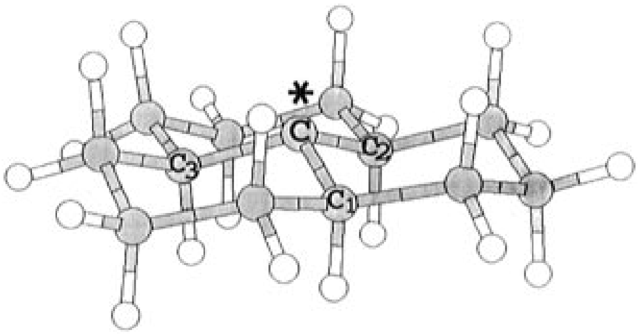

Figure 1. $C_{13}H_{21}$ cluster, which is our most accurate model for the hydrogenated diamond (111) surface. The radical site is denoted by a star.

TABLE 1: Summary of B3LYP Structural Data for CH_3 + FNO_2. Bond Lengths Are in Å and Angles Are in deg. Experimental Values Are Given in Parentheses

compound	symmetry	
CH_3[a]	D_{3h}	C−H = 1.083 (1.079)
CH_3F[b]	C_{3v}	C−F = 1.383 (1.382), C−H = 1.096 (1.090), FCH = 109.6 (108.4)
NO2c	C_{2v}	N−O = 1.203 (1.197), ONO = 133.8 (134.1)
FNO_2[d]	C_{2v}	N−O = 1.189 (1.180), F−N = 1.457 (1.467), FNO = 112.5 (112)
$CH_3\cdots FNO_2$	C_S[e]	C−F = 3.039, F−N = 1.459, N−O = 1.189, C−H_1 = 1.083, C−$H_{2,3}$ = 1.083, FNO = 112.6, FCH_1 = 90.0, $FCH_{2,3}$ = 89.9
CH_3−F−NO_2	C_S[f]	C−F = 2.126, F−N = 1.636, N−O = 1.189, C−H_1 = 1.082, C−$H_{2,3}$ = 1.082, FNO = 112.4, FCH_1 = 95.8, $FCH_{2,3}$ = 96.3

[a] Experimental value from ref 25. [b] Experimental values from ref 26. [c] Experimental values from ref 27. [d] Experimental values from ref 28. [e] Effect of rotation of the nitro group is less than 0.001 Å for bond distances and less than 0.1° for angles. The values refer to the staggered rotational conformer, where the ONO plane is in the plane perpendicular to the FCH_1 plane. H_2 and H_3 are equivalent. [f] Transition state. For the eclipsed conformer bond distances differ less than 0.001 Å, FNO = 112.4, FCH_1 = 96.2, and $FCH_{2,3}$ = 96.0.

2. Model

It is known that the carbon atoms at the surface of a hydrogenated diamond (111) are very close to the positions they would occupy in the bulk.[8] While the C−H bond energies are not known, it is established[8] that high temperatures are required to desorb the hydrogens; clearly, the C−H bond energies are sizeable, as expected. Since C−F bond energies tend to be slightly larger than the analogous C−H bond energies,[9] we expect F to be strongly bound to diamond (111). Ideally one would study the reaction of FNO_2 with a radical site on hydrogenated diamond (111) using a method that includes periodic boundary conditions. However, codes that include periodic boundary conditions are not ideally suited for the location of the barrier and, in general, use either the self-consistent-field (SCF) or density function theory (DFT) approximation. Since barriers tend to be difficult to compute, we want to be able to test the DFT methods using higher levels of theory. The best way to do this is to use a cluster model, and that is the approach that we use. In such an approach the question of the correct cluster size naturally arises. For metals large clusters are required, but on the basis of the similar C−H bond energies for alkanes,[9] we expect rapid convergence of the C−H and C−F bond energies with cluster size, thus making the cluster approach well suited for this problem.

The smallest cluster that we use to model the radical site on diamond (111) is CH_3. Therefore the reaction $FNO_2 + CH_3 \rightarrow NO_2 + CH_3F$ represents our simplest model and is sufficiently small to allow accurate calibration calculations. The C−H and C−F bond energies of CH_4 and CH_3F, respectively, are 2−10 kcal/mol larger than for the molecules with C−C bonds adjacent to the breaking bond. This is because the neighboring C_nH_y groups stablize the radical relative to the H atoms in CH_3. This effect is smaller for F than H since the neighboring C_nH_y groups also help stablize the C−F bond by donating charge to the bonding carbon atom. This donation is the biggest effect missing in our smallest model but is not expected to affect the conclusions of the calibration calculations.

The next larger cluster we use is *tert*-butyl. In this model the C−F bonding site has three CH_3 neighbors, which corrects for the main limitation of the smaller cluster model. On the basis of the C−H bond energies in alkanes, the C−F bond strength is expected to be close to that for F on diamond (111). While the C−F bond energy should be essentially converged for this model, it neglects any steric effects between the surface and NO_2. This limitation is removed in the studies using our largest cluster, $C_{13}H_{21}$, where the neighboring surface atoms are also included—see Figure 1.

3. Methodology

The geometries are fully optimized and the frequencies computed at the optimal geometry using using DFT based on the B3LYP[10] functional. The B3LYP calculations are calibrated using the coupled cluster singles and doubles approach[11] including a correction for unlinked triple excitations,[12] CCSD(T), the internally contracted multireference configuration interaction (ICMRCI) approach[13,14] based on complete-active-space SCF (CASSCF) orbitals, and multireference second-order Möller Plesset perturbation theory[15,16] based on a CASSCF reference (CASPT2). The effect of higher excitations in the ICMRCI approach is estimated using the multireference analog of the Davidson correction and is denoted +Q.

Most calculations are performed using the basis sets developed by Pople and co-workers.[17] Some calculations are performed using the augmented correlation-consistent polarized valence double-ζ (aug-cc-pVDZ) set developed by Dunning and co-workers.[18,19] While the CCSD(T) method is known to yield a very accurate description of the correlation problem, it requires very large basis sets to reach the one-particle basis set limit. To overcome this limitation, we used a modified G2[20] approximation, namely, the G2(B3LYP/MP2/CC) approach.[21] For simplicity, we denote this as G2′(MP2). In this approach the geometry and zero-point energy (ZPE) are determined at the B3LYP level of theory using the 6-31G* basis set; to calculate the zero-point energy the B3LYP harmonic frequences are scaled by 0.98. At this geometry, the energies are calculated at the MP2/6-311G**, MP2/6-311+G(3df,2p), and CCSD(T)/6-311G** levels of theory. The final energy, E(G2′(MP2)), is obtained as E(CCSD(T)/6-311G**) + E(MP2/6-311+G(3df,-2p)) − E(MP2/6-311G**)+ZPE+HLC, where HLC is the higher level correction, which is based on the number of valence α and β electrons and determined by minimizing the computed error in the atomization energies of 55 molecules where the experimental values are well-known.

The ICMRCI and CASPT2 calculations have been performed using the MOLPRO code,[13,14,22,23] while other studies were performed using the GAUSSIAN 94 package of computer programs.[24]

4 Results and Discussion

4.1. CH_3 + FNO_2. The B3LYP structures for the reaction of CH_3 + FNO_2 are given in Table 1. The harmonic frequencies confirm the identification of the structures as minima or as a transition state. Also included are the experimental geo-

TABLE 2: Calibration Calculations for Bond Dissociation Energies (D_e and D_0) and Relative Energies ΔE_e for the Reaction $CH_3 + FNO_2$[a]

	D_e (kcal/mol)			
structure	B3LYP	CCSD(T)[b]	CCSD(T)+ΔMP2	G2′(MP2)
CH_3-H	113.15	109.06	110.50	113.21
CH_3-F	113.00	105.21	114.62	117.32
NO_2-F	57.84	47.10	56.15	58.86
ONO−H trans	77.02	80.67	83.54	86.25
ONO−H cis	78.01	81.00	83.05	85.76
NO_2-H	71.83			

	D_0 (kcal/mol)		
structure	B3LYP	G2′(MP2)	expt[c]
CH_3-H	103.68	103.74	103.30
CH_3-F	107.06	111.38	108.20
NO_2-F	54.77	55.79	51.65
ONO−H trans	69.96	79.19	77.59
ONO−H cis	70.93	78.68	77.07

	ΔE_e (kcal/mol)		
structure	B3LYP	CCSD(T)[b]	CCSD(T)+ΔMP2
$CH_3 + FNO_2$	0.00	0.00	0.00
$CH_3\cdots FNO_2$[d]	−0.40	−0.17	−0.22
CH_3-F-NO_2[e]	4.35	11.85	12.35
$CH_3F + NO_2$	−55.17	−58.11	−58.47

[a] The B3LYP values are computed with the 6-31G* basis set and CCSD(T) calculations use the 6-311G**. ΔMP2 is the MP2 basis set incompleteness contribution to the G2′(MP2) approach. The G2′(MP2) approach is described in the text. [b] Computed at the B3LYP optimized geometry. [c] Experimental values from ref 27. [d] Prereaction adduct. [e] Transition state.

TABLE 3: Summary of Multireference-Based Calculations for the Barrier Height of the Transition State $CH_3 + FNO_2$ Reaction[a]

	method		
reference	CAS	CASPT2	ICMRCI+Q
(3/3)[b]	18.91	5.03	11.54
(3/3)[c]	18.91	6.47	12.09
(7/7)-0.02[c]	20.61	6.49	11.57

[a] The calculations are performed using the aug-cc-pVDZ basis set. In the calculation denoted by (3/3) the three electrons occupying the binding orbitals C−F(a′) or N−F(a′) are active and distributed in three a′ orbitals. In the (7/7)-0.02 calculation, seven electrons are distributed in seven a′ orbitals in all possible ways selecting reference configuration with coefficients larger than 0.02 of the zeroth-order CASSCF wave function. [b] All valence electrons correlated in the CASPT2 and ICMRCI calculations. [c] The F and O 2s electrons not correlated.

metries[25−28] for the reactants and products. Overall the B3LYP geometries are in good agreement with experiment as has been found for many other cases.[29]

As noted above we calibrate the energetics at the B3LYP level using more accurate approximations; the results of these calibration calculations are summarized in Tables 2 and 3. We first consider some of the relevant D_e values in Table 2. The G2′(MP2) values are expected to be the most accurate as they are based on the CCSD(T) approach but include corrections for basis incompleteness and residual errors. In general, the B3LYP bond dissociation energies are in good agreement with the G2′(MP2) results. In fact, the average absolute difference between the B3LYP and G2′(MP2) results is smaller than the difference between CCSD(T) and G2′(MP2). This is encouraging because the B3LYP calculations are significantly less costly than the CCSD(T) ones. The difference between the CCSD(T)+ΔMP2 and G2′(MP2) results shows that the MP2 estimate for the basis set incompleteness is more important than the higher level correction. We also compare the computed D_0 values with experiment[27] in Table 2. While the average absolute error in the B3LYP approach is about twice that of the G2′(MP2) approach, it still acceptable especially considering that the largest errors are for HNO_2, which is only considered to demonstrate that the NO_2 radical, once formed, will not abstract H from the diamond (111) surface. The CH_3-F and NO_2-F bond energies confirm that the same is true for the F atoms bonded to the surface.

In the bottom of Table 2 the relative energetics of the reaction

$$FNO_2 + CH_3 \rightarrow NO_2 + CH_3F$$

are compared for the three levels of theory. As for the bond energies, the B3LYP values are in good agreement with the CCSD(T)+ΔMP2 approach, excluding the barrier height, where the B3LYP value is significantly smaller than either the CCSD(T) or CCSD(T)+ΔMP2 results. It is interesting that while the B3LYP does not accurately describe the barrier, it does yield results very similar to the higher levels of theory for the weakly bound $CH_3\cdots FNO_2$ complex.

As noted above, barrier heights are difficult to compute accurately. At the CCSD(T) level, the MP2 correction for one-particle basis set incompleteness is only 0.5 kcal/mol, suggesting that the barrier height is not strongly affected by further improvements in the basis set. To test if the single reference based CCSD(T) approach is correctly describing the barrier height, we perform multireference-based calibration calculations that are summarized in Table 3. Since it is not possible to perform a correlated calculation based on a full valence CASSCF calculation, we consider smaller active spaces. The first has only the three electrons directly involved in the reaction; for the reactants this is the CH_3 open-shell electron and F−N bond, while for the products this is the C−F bond and the NO_2 open-shell electron. These three electrons are distributed in three active orbitals. While the CASSCF value is too large, the ICMRCI+Q value is in good agreement with the CCSD(T) result. The CASPT2 value is smaller. Removing the F and O 2s electrons from the correlation problem does not significantly affect the result, nor does expanding the active space. On the basis of the agreement between the CCSD(T) and IMRCI+Q results, we conclude that the best estimate for the barrier is about 12 kcal/mol (13 kcal/mol including the B3LYP zero-point energies). Thus while the B3LYP yields reasonable bond energies, the barrier is too small; however, it is sufficiently accurate that we can establish the trends in the barrier with improving the quality of the model for diamond (111).

4.2. FNO_2 + *tert*-Butyl and $C_{13}H_{21}$.

Fully optimized structures for the reactions

$$FNO_2 + C(CH_3)_3 \rightarrow NO_2 + F-C(CH_3)_3 \qquad (2)$$

$$FNO_2 + C_{13}H_{21} \rightarrow NO_2 + F-C_{13}H_{21} \qquad (3)$$

are given in Table 4. As note above, $C_{13}H_{21}$ (see Figure 1) is our best model for a hydrogenated diamond film. The C−C distances in $C_{13}H_{21}$ are generally longer and C_1CC_2 bond angles are somewhat smaller than found for *tert*-butyl. That is, without the second shell of carbon atoms to constrain the geometry, *tert*-butyl becomes more planar. This is due the larger relaxation. However, this effect is relatively small, with the central carbon in $C_{13}H_{21}$ being 0.23 Å above the $C_1C_2C_3$ plane compared with 0.16 Å *tert*-butyl. The C−F bond distances in the products with $C_{13}H_{21}$ and *tert*-butyl are similar to each other and only slightly longer than for CH_3F, where there are no neighboring C−C bonds. The transition state shows a larger variation with model; there is a general lengthening of the C−F

TABLE 4: B3LYP Structural Data for the Reaction of *tert*-Butyl and $C_{13}H_{21}$ with FNO_2 (Bond Lengths in Å, Angles in deg)[a]

compound	symmetry	
$(CH_3)_3C$	C_{3v}	$C-C_{123} = 1.498$, $C_1CC_2 = 118.9$, $\kappa = 0.158$
$(CH_3)_3CH$	C_{3v}	$C-H = 1.101$, $C-C_{123} = 1.535$, $HCC_1 = 107.8$, $C_1CC_2 = 111.1$, $\kappa = 0.469$
$(CH_3)_3CF$	C_{3v}	$C-F = 1.416$, $C-C_{123} = 1.527$, $FCC_1 = 106.5$, $C_1CC_2 = 112.2$, $\kappa = 0.434$
$(CH_3)_3C-F-NO_2$[b]	C_s[c]	$C-F = 2.371$, $F-N = 1.568$, $C-C_1 = 1.496$, $C-C_{23} = 1.495$, $NO = 1.189$, $FNO = 112.6$, $FCC_1 = 95.4$, $FCC_2 = 96.2$, $C_1CC_2 = 118.7$, $C_3CC_2 = 119.3$, $\kappa = 0.156$
$(CH_3)_3C\cdots FNO_2$	C_s[c]	$C-F = 2.750$, $F-N = 1.476$, $C-C_1 = 1.497$, $C-C_{23} = 1.497$, $NO = 1.189$, $FNO = 112.6$, $FCC_1 = 94.6$, $FCC_2 = 96.2$, $C_1CC_2 = 119.0$, $C_3CC_2 = 119.2$, $\kappa = 0.146$
$C_{13}H_{21}$	C_s	$C-C_1 = 1.515$, $C-C_{23} = 1.514$, $C_1CC_2 = 117.7$, $C_2CC_3 = 117.7$, $\kappa = 0.231$
$C_{13}H_{21}H$	C_s	$C-H = 1.106$, $C-C_1 = 1.547$, $C-C_{23} = 1.546$, $HCC_1 = 107.2$, HCC_2 107.2, $C_1CC_2 = 111.6$, $C_2CC_3 = 111.6$, $\kappa = 0.458$
$C_{13}H_{21}F$	C_s	$C-F = 1.427$, $C-C_1 = 1.544$, $C-C_{23} = 1.543$, $FCC_1 = 106.5$, $FCC_2 = 106.6$, $C_1CC_2 = 112.2$, $C_2CC_3 = 112.2$, $\kappa = 0.440$
$C_{13}H_{21}-F-NO_2$[b]	C_s[c]	$C-F = 2.536$, $F-N = 1.541$, $C-C_1 = 1.513$, $C-C_{23} = 1.513$, $NO = 1.188$, $FNO = 112.4$, $FCC_1 = 97.9$, $FCC_2 = 98.6$, $C_1CC_2 = 118.0$, C_2CC_3 117.8, $\kappa = 0.220$

[a] κ denotes the distance from the central carbon atom C to the $C_1C_2C_2$ plane. These atoms are numbered such that C_1 is on the symmetry plane for C_s structures (Figure 1). [b] Transition state. [c] The rotation of the nitro group is essentially free (energy differences for rotational conformers less than 0.1 kcal/mol). The structures refer to the staggered rotational conformer, where the NO_2 plane is in the plane perpendicular to the NCC_1 plane.

TABLE 5: Relevant Bond Energies and Energetics (kcal/mol) for the Reaction of FNO_2 with CH_3, *tert*-Butyl, and $C_{13}H_{21}$ Computed at the B3LYP Level

	D_e	D_0
H_3C-H	113.15	103.68
$(H_3C)_3C-H$	100.53	91.10[a]
$C_{13}H_{21}-H$	101.82[b]	
H_3C-F	113.00	107.06
$(H_3C)_3C-F$	115.32	111.08
$C_{13}H_{21}-F$	117.44[c]	

	$X = CH_3$	$X = C(CH_3)_3$		$X = C_{13}H_{21}$
	ΔE_e	ΔE_e	ΔE_0	ΔE_e
$X + FNO_2$	0.00	0.00	0.00	0.00
$X\cdots FNO_2$[d]	−0.40	−1.02		
$X-F-NO_2$[e]	4.35	−0.55	−0.85	−2.81
$XF + NO_2$	−55.17	−57.48	−56.31	−59.60

[a] Experimental value from ref 9 is 93.2 kcal/mol. [b] The D_e value is 103.77 kcal/mol if only the central atom in $C_{13}H_{21}$ is allowed to relax. [c] The D_e value is 119.39 kcal/mol if only the central atom in $C_{13}H_{21}$ is allowed to relax. [d] Prereaction adduct. [e] Transition state.

bond and contraction of the F−N bond. These changes are consistent with the flat potential at a transition state.

The relevant bond energies and energetics for reactions 2 and 3 are summarized in Table 5. The C−H bond energies for *tert*-butyl and $C_{13}H_{21}$ are significantly smaller than for CH_3 as expected, because the surrounding C−C bonds stabilize the radical. The values for *tert*-butyl and $C_{13}H_{21}$ are very similar because the second nearest neighbors have only a very small effect on the C−H bond strength of the central carbon, which is consistent with alkane binding energies. The C−F bond energies show the opposite trend; namely, the bond energies are increasing with cluster size, which suggests that the neighboring C_nH_m groups are stabilizing the C−F bond by more than the radical. This difference between H and F is consistent with the polarity of the C−F bond. We also note that while the C−H bond energies are smaller than for CH_3 the model still supports the claim that NO_2 will not abstract an H atom from the diamond surface.

Our cluster model assumes that there is complete freedom to relax the geometry; however, this not completely true as the F deposition site is really part of an infinite surface. We test the importance of this effect by only relaxing the central C in $C_{13}H_{21}$. It has previously been argued[30] that a partial optimization restricted to relaxation of the central C-atom introduces only small errors. Our results are consistent with this; the C−H and C−F bond energies differ by only 1.9 kcal/mol between the fully and partly relaxed models.

The increase in the C−F bond strength with cluster size means that the exothermicity of the reaction is also increasing with cluster size—see Table 5. Consistent with Hamonds postulate, this results in a lowering of the barrier. In fact, for *tert*-butyl and $C_{13}H_{21}$ the barrier is now below the reactants and only slightly above the weakly bound complex. However as demonstrated above, the B3LYP barrier is too low. If we correct the values for the larger clusters using the results from the calibration calculations, we estimate that the barrier on diamond (111) will be about 10 kcal/mol. This barrier is sufficiently small that FNO_2 should deposit F atoms at the radical sites at reasonable temperatures.

Using the $C_{13}H_{21}$ cluster, we have computed the C−NO_2 bond energy to be about 50 kcal/mol.[31] This is sufficiently large that if NO_2 encounters a radical site, it will bond. Thus the addition of F to radical sites using FNO_2 can only be used for low concentrations of the surface radicals, such that the NO_2 once formed will carried away before it reacts. Thus writing data on a surface would have to involve many passes across the surface, with only a few surface radicals formed between each exposure of the surface to FNO_2. It would then be desirable to read the surface and eliminate any surface NO_2 molecules and react the radical site with FNO_2 to deposit a F atom. Thus writing with FNO_2 would be a slow process, but it does seem to avoid the problem of radicals destroying the data as it is written.

5. Summary and Conclusions

The calibration calculations show that the B3LYP bond energies should be reasonably accurate but that the barrier heights at this level are too low. The C−F and C−H bond dissociation energies for X−$C_{13}H_{21}$ have been determined at the B3LYP level to model the surface bonding on a diamond (111) surface. The values are only 1−2 kcal above the values for *tert*-butyl. The calculations show that NO_2 can not abstract a F or H from the surface. The barrier for the reaction of the surface with FNO_2 is found to have about a 10 kcal/mol barrier, after including a correction to account for limitations in the B3LYP approach. The difference in barrier between $C_{13}H_{21}$ and *tert*-butyl shows that the effect of the second nearest neighbors is small.

References and Notes

(1) Mamin, H. J.; Terris, B. D.; Fan, L. S.; Hoen, S.; Barrett, R. C.; Rugar, D. *IBM J. Res. Dev.* **1995**, *39*, 681.

(2) Eigler, D. M.; Schweizer, E. K. *Nature* **1990**, *344*, 524−526.

(3) Cho, K.; Joannopoulos, J. D. *Phys. Rev. B* **1996**, *53*, 4553.

(4) Bauschlicher, C. W.; Ricca, A.; Merkle, R. *Nanotechnology*, in press.

(5) Avouris, Ph.; Walkup, R. W.; Rossi, A. R.; Akpati, H. C.; Nordlander, P.; Shen, T.-C.; Lyding, J. W.; Abeln, G. C. *Surf. Sci.* **1996**, *363*, 368.

(6) Smentkowski, V. S.; Yates, J. T. *Science* **1996**, *271*, 193.

(7) Geis, M. W.; Angus, J. C. *Sci. Am.* **1992**, *267* (4), 84.

(8) Pate, B. B. *Surf. Sci*. **1986**, *165*, 83.

(9) McMillen, D. F.; Golden, D. M. *Annu. Rev. Phys. Chem*. **1982**, *33*, 493.

(10) Stevens, P. J.; Devlin, F. J.; Chablowski, C. F.; Frisch, M. J. *J. Phys. Chem*. **1994**, *98*, 11623.

(11) Bartlett, R. J. *Annu. Rev. Phys. Chem*. **1981**, *32*, 359.

(12) Raghavachari, K.; Trucks, G. W.; Pople, J. A.; Head-Gordon, M. *Chem. Phys. Lett*. **1989**, *157*, 479.

(13) Werner, H. J.; Knowles, P. *J. Chem. Phys*. **1988**, *89*, 5803.

(14) Knowles, P. J.; Werner, H. J. *Chem. Phys. Lett.* **1988**, *145*, 514.

(15) Andersson, K.; Roos, B. O. *Modern Electronic Structure Theory*; Yarkony, D. R., Ed.; World Scientific Publishing Company: Singapore, 1995; p 55.

(16) Werner, H. J. *Mol. Phys*. **1996**, *89*, 645.

(17) Frisch, M. J.; Pople, J. A.; Binkley, J. S. *J. Chem. Phys*. **1984**, *80*, 3265 and references therein.

(18) Dunning, T. H., Jr. *J. Chem. Phys.* **1989**, *90*, 1007.

(19) Kendall, R. A.; Dunning, T. H.; Harrison, R. J. *J. Chem. Phys*. **1992**, *96*, 6796.

(20) Curtiss, L. A.; Raghavachari, K.; Trucks, G. W.; Pople, J. A. *J. Chem. Phys.* **1991**, *94*, 17221.

(21) Bauschlicher, C. W.; Partridge, H. *J. Chem. Phys*. **1995**, *103*, 1788.

(22) Werner, H. J.; Knowles, P. *J. Chem. Phys*. **1985**, *82*, 5053.

(23) Knowles, P. J.; Werner, H. J. *Chem. Phys. Lett.* **1985**, *115*, 259.

(24) Frisch, M. J.; Trucks, G. W.; Schlegel, H. B.; Gill, P. M. W.; Johnson, B. G.; Robb, M. A.; Cheeseman, J. R.; Keith, T.; Petersson, G. A.; Montgomery, J. A.; Raghavachari, K.; Al-Laham, M. A.; Zakrzewski, V. G.; Ortiz, J. V.; Foresman, J. B.; Cioslowski, J.; Stefanov, B. B.; Nanayakkara, A.; Challacombe, M.; Peng, C. Y.; Ayala, P. Y.; Chen, W.; Wong, M. W.; Andres, J. S.; Replogle, E. S.; Gomperts, R.; Martin, R. L.; Fox, D. J.; Binkley, J. S.; Defrees, D. J.; Baker, J.; Stewart, J. P.; Head-Gordon, M.; Gonzalez, C.; Pople, J. A. Gaussian 94, Revision D.1; Gaussian, Inc.: Pittsburgh, PA, 1995.

(25) Herzberg, G. *Molecular Spectra and Molecular Structur*; Van Nostrand Reinhold Company: New York, 1966; Vol. III.

(26) Duncan, J. L. *J. Mol. Spectrosc.* **1976**, *60*, 225.

(27) Chase, M. W.; Davies, C. A.; Downey, J. R.; Frurip, D. J.; McDonald, R. A.; Syverud, A. N. *J. Phys. Chem. Ref. Data* **1985**, *14* (Suppl. 1).

(28) Harmony, M. D.; Laurie, V. W.; Kuczkowski, R. L.; Schwendemann, R. H.; Ramsey, R. H.; Lovas, F. J.; Lafferty, W. J.; Maki, A. G. *J. Phys. Chem. Ref. Data* **1979**, *8*, 619.

(29) Bauschlicher, C. W.; Partridge, H. *Chem. Phys. Lett*. **1995**, *240*, 533.

(30) Larsson, K.; Lunell, S.; Carlsson, J.-O. *Phys. Rev. B.* **1993**, *48*, 2666.

(31) Thümmel, H. T. To be published.